Computer Assisted Mechanics and Engineering Sciences, 13: 593–611, 2006.

Non-statistical physically reasonable technique for a posteriori estimation of experimental data error

Jacek Magiera
Institute for Computational Civil Engineering, Cracow University of Technology
ul. Warszawska 24, 31-155 Kraków, Poland

(Received in the final form November 28, 2006)

In the paper presented is an application of the physically based global method (PBGM) to a posteriori estimation of experimental data error. It is proposed here to build data error measures by spanning a high quality physically reasonable smoothing fit to data and treat it as a reference field for error estimation in a very similar way it is done in the postprocessing type error estimates used widely in FE or meshless methods, where the higher order (superconvergent) solutions are used for building error estimates (post-processing type of error estimators). The new technique is different from classical methods of experimental data error estimation as it provides non-statistical estimates of the data error and as such it may be applied to a wider range of problems, including cases when only a single data set is available (e.g., destructive testing). And because the new approach builds the estimates while performing its standard physically based global-type approximation, it fully integrates other features of the PBGM approach like data interpolation, extrapolation or differentiation. In the paper the whole PBGM approach is presented, including the concept of the method formulated for the case of analysis of residual stress in railroad rails, discretisation with MFDM, then several PBGM a posteriori error estimates are introduced and results for test problems (benchmark and actual data) are shown.

Keywords: hybrid methods, physically based approximation, meshless finite differences method, smoothing of experimental data, error estimation techniques

1. Introduction

Present-day experimental testing requires not only sophisticated instruments or qualified personnel but advanced data analysis techniques as well. Such data analysis techniques are expected to provide high quality results and guarantee speed and reliability. Their successful application requires that such techniques offer not only simple data manipulation capabilities, but also have power for data enhancement and enrichment like smoothing, interpolation and/or extrapolation, differentiation, mapping, contour lines plotting, automatic quality assessment, error analysis and self-controllability. Unfortunately, the methods applied classically for analysis and enhancement of the experimental data are usually oriented on performing one particular task (e.g., there are methods for building data statistics, but they do not offer interpolating or differentiating capabilities), in majority of cases they require several (or more) independent data series and if there is a need for performing several of the tasks listed above (e.g. if one wants to smoothen the data first, then differentiate it and extrapolate to a region where there were no measurements taken), they are performed as a sequence of independent actions and with use of independent tools. Those tools are usually not coordinated with each other and might offer different level of accuracy. In such cases, the quality of the final results might be questioned.

To meet the challenge and requirements imposed by the modern experimental data processing, a new methodology was proposed and developed into a stand-alone approach called as the physically based approximation of experimental data by the global method (PBGM) [7, 10]. It was devised in such a way that it has all the features required for data enhancement and analysis, offering high quality, physically based smoothing capabilities and being able at the same time to perform data

mapping, interpolation, extrapolation, differentiation or integration. Thanks to such a potential it also lends itself well for providing a posteriori estimates of actual experimental data error [11, 12]. To its credit, all these capabilities are possible without any sort of statistical analysis.

2. Physically based approximation

The term "physically based" (PB) approximation [7] is understood here as a method of building fits to data that takes into account – in a weighted manner – all information available for the considered problem. The relations that can contribute valuable information may have theoretical, experimental, statistical and/or heuristic roots and they may come in the form of either global or local, algebraic, integral or differential types. Moreover, they may be formed as equalities or inequalities.

There is no one definite way to build physically based approximation so its very concept may lead to many formulations. In general, all of them may be divided into local or global ones. Local formulations are those that offer fits only at one point at a time (a step-by-step procedure; see e.g., global-local method (GLM) by Karmowski [5, 7]). If a formulation makes it possible to build a fit at all points of interests in a considered domain at the same time, such a procedure will be called as the physically based global method (PBGM). The global formulation has an advantage over the local formulation as it permits easy incorporation of almost any type of theoretical relations, including boundary conditions of any type – both local and global, as well as all kinds of differential and/or integral relations.

2.1. The global method

The implementation of the global method is based on a variational stress-type formulation proposed in [7]. It was posed as a nonlinear constrained minimization problem. The general concept is as follows.

Find such a distribution of $\boldsymbol{\sigma}$ in the examined domain A which minimises the following hybrid theoretical-experimental functional $\Phi(\boldsymbol{\sigma}, \lambda)$[1],

$$\min_{\boldsymbol{\sigma}} \Phi(\boldsymbol{\sigma}, \lambda) = \lambda \Phi^{\mathrm{T}}(\boldsymbol{\sigma}) + (1 - \lambda)\, \Phi^{\mathrm{E}}(\boldsymbol{\sigma}), \qquad \lambda \in [0, 1], \tag{1}$$

satisfying certain equality

$$A(\boldsymbol{\sigma}) = 0, \tag{2}$$

and inequality constraints

$$B(\boldsymbol{\sigma}) \leq \Delta f(\boldsymbol{\sigma}), \tag{3}$$

where $\Delta f(\boldsymbol{\sigma})$ are admissible error tolerances[2] and λ is a scalar weighting parameter.

The theoretical part $\Phi^{\mathrm{T}}(\boldsymbol{\sigma})$ of the hybrid functional in Eq. (1), expresses certain variational/integral demands that the approximated field is required to obey. They might be known from the physics of the investigated phenomenon or might be a demand of heuristic roots, like for instance, smoothness of the approximated field. In the considered here case oriented on analysis of

[1] a typical multi-criteria optimisation formulation is used here

[2] usually, they are treated as estimates of an average error of the experimental technique applied; they may have different meaning (local or global) depending on the particular inequality type used

residual stress in railroad rails [13], the average Karmowski's curvature of the stress field as [6] was chosen as the $\Phi^{\mathrm{T}}(\boldsymbol{\sigma})$,

$$\Phi^{\mathrm{T}}(\boldsymbol{\sigma}) = \int_A^{\kappa^2(\boldsymbol{\sigma})} \mathrm{d}A. \tag{4}$$

In the Cartesian coordinate system it is expressed as

$$\kappa^2(\sigma_{ij}) = \frac{1}{2\pi} \int_0^{2\pi} \frac{\partial^2 \sigma_{ij}}{\partial \nu^2} \frac{\partial^2 \sigma_{ij}}{\partial \nu^2} \, \mathrm{d}\phi, \tag{5}$$

in which a product of the directional second derivatives $\frac{\partial^2}{\partial \nu^2}$ of the stress tensor σ_{ij}, differentiated along a given vector ν inclined under angle ϕ to the axis OX, is integrated over all possible directions ϕ from $[0, 2\pi]$.[3]

The experimental part of the functional $\Phi^{\mathrm{E}}(\boldsymbol{\sigma})$ is chosen as

$$\Phi^{\mathrm{E}}(\boldsymbol{\sigma}) = \frac{1}{K} \sum_{k=1}^{K} \Xi \left(\frac{f(\sigma_{ij}^k) - f(\overline{\overline{\sigma}}_{ij}^k)}{\Delta f(\sigma_{ij}^k)} \right), \qquad i,j = 1,2,3, \tag{6}$$

where $f(\sigma_{ij}^k)$ is the approximated stress field to be found at the point k, $f(\overline{\overline{\sigma}}_{ij}^k)$ is the experimentally determined stress field at that point and $\Delta f(\sigma_{ij}^k)$ is a local weighting factor ascribed to that data point (which reflects a local credibility of the data). The function Ξ is the probability distribution function that describes statistics of the measurements while the function $f$is a function mapping the stress subspace into the subspace of the originally recorded quantities[4].

The influence of the theoretical $\Phi^{\mathrm{T}}(\boldsymbol{\sigma})$ and experimental $\Phi^{\mathrm{E}}(\boldsymbol{\sigma})$ parts of the hybrid functional $\Phi(\boldsymbol{\sigma}, \lambda)$ on the final results is weighted out by a scalar parameter λ which optimal value is not known *a priori* and has to be found iteratively.

The equality constraints $A(\boldsymbol{\sigma}) = 0$ usually express certain physical laws that have to be satisfied exactly while the inequality constraints $B(\boldsymbol{\sigma}) \leq \Delta f(\boldsymbol{\sigma})$ usually come from the experimental area and in general express data uncertainty (admissible experimental error tolerances). In the considered here case of residual stress in rails, the equality constraints were chosen as

- internal equilibrium equations (self-equilibrated)

$$\sigma_{ij,j} = 0 \qquad \text{in } A, \tag{7}$$

- local boundary conditions (residual stress, no loading at the boundary)

$$\sigma_{ij} n_j = 0 \qquad \text{on } \partial A, \tag{8}$$

- global boundary conditions (total forces and momentum for a self-equilibrated stress field)

$$\int_A \sigma_{xx} \, \mathrm{d}A = 0, \qquad \int_A \sigma_{yy} \, \mathrm{d}A = 0, \qquad \int_A [(\sigma_{xx} + \sigma_{yx})y - (\sigma_{yy} + \sigma_{xy})x] \, \mathrm{d}A = 0. \tag{9}$$

In the current implementation the inequality constraints $B(\boldsymbol{\sigma}) \leq \Delta f(\boldsymbol{\sigma})$ were imposed as

- local tolerances of experimental error

$$\left| f(\sigma_{ij}^k) - f(\overline{\overline{\sigma}}_{ij}^k) \right| \leq \Delta f(\sigma_{ij}^k), \qquad i,j = 1,2, \quad k = 1,K, \tag{10}$$

[3]thanks to this definition the Karmowski's curvature is invariant with respect to the rotation of the coordinate system

[4]stress field is directly immeasurable; in experimental studies, there are other quantities (displacements, strains, etc.) that are determined so for the stress type formulation developed here a mapping functions between the stress and the other subspaces is required

- global tolerance of experimental error

$$\sqrt{\sum_{i,j=1}^{2} \frac{1}{K} \sum_{k=1}^{K} \frac{\left[f(\sigma_{ij}^k) - f(\bar{\sigma}_{ij}^k)\right]^2}{\left[\Delta f(\sigma_{ij}^k)\right]^2}} \leq \Delta f(\boldsymbol{\sigma})_{\text{global}}\,, \tag{11}$$

where $\Delta f(\boldsymbol{\sigma})_{\text{global}}$ is bound to an average non-dimensional estimate of the accuracy of the experimental method applied during testing. In Eq. (11) the probability distribution function Ξ of Eq. (6) has been substituted by its second-order polynomial approximation, which leads to a least square type formulation of the experimental part.

The general formulation (1)–(11) given above lacks, at the moment, any sort of procedure for determining a proper value of the weighting factor λ. Several solutions to this problem were considered in [7], in the current implementation adopted was a two-stage optimization procedure:

Stage I: For a given value of the parameter λ, find the stationary point $\boldsymbol{\sigma}(\lambda)$ of the functional (1)

$$\min_{\boldsymbol{\sigma}} \Phi(\boldsymbol{\sigma}, \lambda) = \lambda \Phi^{\mathrm{T}}(\boldsymbol{\sigma}) + (1-\lambda)\Phi^{\mathrm{E}}(\boldsymbol{\sigma}), \qquad \lambda \in [0,1], \tag{12}$$

satisfying exactly all equality constraints $A(\boldsymbol{\sigma}) = 0$, Eqs. (7)–(9).

Stage II: Find

$$\min_{\lambda} \lambda, \qquad \lambda \in [0,1], \tag{13}$$

for which the λ-dependent solution family for $\boldsymbol{\sigma}(\lambda)$ fulfils one (or more) of the constraints $B(\boldsymbol{\sigma}) \leq \Delta f(\boldsymbol{\sigma})$ in the form of equality, and none of the rest is violated at any other experimental points k of the considered domain A.

From the numerical point of view, the process of arriving at the final solution is iterative. Parameter λ is being searched in the interval $(0,1)$[5] in such a way that it is initially assumed to be equal to a starting value $\lambda_0$and then the Stage I minimization problem (1) is solved. If for this value inequalities (10)–(11) are not violated, it is increased by an assumed value of $\Delta\lambda$. Otherwise, λ is reduced by $\Delta\lambda$and the iteration is carried out again[6]. The procedure breaks off when one (or more) of the inequality constraints (10)–(11) is satisfied in the form of equality at a point or a set points simultaneously with an assumed violation tolerance τ.[7]

2.2. Discretisation of the global method

Discrete formulation of the global method was obtained by application of the meshless finite difference method (MFDM) [10, 14]. This choice was driven by the fact that it was considered to be the best approach to suit the needs of transformation of the variational formulation, Eqs. (1)–(13) into a numerical procedure. The following considerations list competitive advantages of a meshless finite difference method over other methods:

[5] the interval is open as $\lambda = 0$ or $\lambda = 1$ would deprive the hybrid functional (1) of one of its mutually counter playing parts, either theoretical ($\lambda = 0$) or experimental ($\lambda = 1$)

[6] of course, after each increase or decrease, the new value of λ is checked whether it still belongs to the admissible interval $(0,1)$; if so, the step $\Delta\lambda$ would be automatically diminished by a half. It would be also diminished by a half if after performing the Stage I calculations and examining the constraints (10)–(11) there was a change in constraints violation status (i.e. if none of them was violated for a previous value of the λ, but after increase by $\Delta\lambda$one or more has been violated or, in opposite case, if the parameter λ has been decreased due to a former violation of a constraint(-s) and this decrease has changed the violation status into the non-violation state)

[7] a small number, usually set to 0.001 in actual computations

1. from the computational point of view the global method requires a non-standard treatment as it involves operation on two separate grids of points, i.e., experimental, at which measurements were collected and over which there is little control[8], and computational, at which approximation process is being performed. Those grids are usually spatially not related to each other, have different densities, certain points that belongs to one of those grid may fall very close to locations of points of the second grid, but there might be areas in the computational grid where no experimental data was collected. The finite element approximation with its stiff topological requirements and difficulty in covering the area with a second, often topologically impaired, mesh does not seem to be compatible with the PBGM formulation;

2. the MFDM is very flexible in discretising both local (strong) and global (weak) formulations and different kind of theoretical relations can be easily incorporated into the final set; again, the way in which the FE approximation is built may limit the freedom of mixing various relations/requirements that may seem to be valuable for analysis of data;

3. the MFDM is very flexible in providing derivatives of the analysed fields of almost any order and with respect to this, it again has a clear advantage over the FE approach;

4. the MFDM approach employs the MWLS-type approximation for building the FD operators which is in a natural way compatible with the least squares approach for building the experimental part of the hybrid functional (1) and the global constraints (11).

Of course, similar flexibility as the MFDM have other meshless methods but their algorithms are often more elaborate and CPU-intensive so in the case of iterative procedure solving many times possibly large problems such formulations did not seem to be the best.

The starting point for the discretisation process is formulation of the physically reasonably finite difference (FD) operators[9]. In order to do that the stress function (2D elastic case considered) was assumed as a polynomial of an appropriate order[10],

$$F(x,y) = a + bx + cy + dx^2 + exy + fy^2 + \cdots + py^4 \tag{14}$$

and then the in-plane stress components σ_{xx}, σ_{yy}, σ_{xy} are classically expressed as

$$\sigma_{xx} = \frac{\partial^2 F}{\partial y^2}, \qquad \sigma_{yy} = \frac{\partial^2 F}{\partial x^2}, \qquad \sigma_{xy} = -\frac{\partial^2 F}{\partial x \partial y}, \tag{15}$$

which leads to the following approximations for the stress components,

$$\begin{aligned} \sigma_{xx} &= 2f + 2ix + 6jy + 2mx^2 + 6nxy + 12py^2, \\ \sigma_{yy} &= 2d + 6gx + 2hy + 2my^2 + 6lxyx + 12kx^2, \\ \sigma_{xy} &= -e - 2hx - 2iy - 3lx^2y - 4mxy - 3nxy^2. \end{aligned} \tag{16}$$

Now, let us build an error functional $\Psi(d,e,f,\ldots,p)$ which will evaluate, in the moving weighted least squares sense [9], the error of approximation at the consecutive nodes of the star for all stress components at those nodes,

$$\Psi(d,e,\ldots,p) = \sum_{k=1}^{N_{\text{star}}} w^2(\rho_k) \left[(\sigma_{xx}^k - \bar{\bar{\sigma}}_{xx}^k)^2 + (\sigma_{yy}^k - \bar{\bar{\sigma}}_{yy}^k)^2 + 2(\sigma_{xy}^k - \bar{\bar{\sigma}}_{xy}^k)^2 \right], \tag{17}$$

[8] as it is delivered by the experimental team and the data analyst may have no chance to interact with them when this grid is created (or particular features of experimental technique used may limit flexibility in creating the experimental grid)

[9] by physically reasonable FD operator it is understood here that the operator being built is to obey part or all of the physical laws valid for the considered problem; the demonstrated here FD operator will satisfy the internal equilibrium equations in the plane stress case

[10] here the case of 4th order stress function approximations will be shown but the PBGM code implements even higher order polynomials

where N_{star} is the total number of nodes in the considered star, w is a weighting function dependent on the distance ρ_k between the central node and the k-th node in the star, $\bar{\bar{\sigma}}^k_{xx}$ is the value of a stress component measured experimentally at that node k and σ^k_{ij} is the value of a stress component evaluated at that node by approximation spanned from the central node. The weighting function was chosen as an inverse distance function,

$$w^2(\rho_k) = \left(\frac{1}{\rho_k^2}\right)^3 = \left[(x_k - x_0)^2 + (y_k - y_0)^2\right]^{-3}. \tag{18}$$

Minimization of the functional (20) with respect to the unknown parameters $\mathbf{u}^T = (d, e, f, \ldots, p)$ leads to a set of linear equations

$$\mathbf{A}\mathbf{u} = \mathbf{B} \tag{19}$$

where $\mathbf{A}$ is a matrix depending only on the relative – with respect to the central node – coordinates of the consecutive nodes of the star and $\mathbf{B}$ is a matrix depending also on the values of the nodal stresses σ^k_{ij}. It is worth emphasizing that the nodal values are not known yet and that in fact they are the basic unknowns for the whole problem. Solving formally the set (19) we obtain

$$\mathbf{u} = \mathbf{A}^{-1}\mathbf{B} \tag{20}$$

where the matrix $\mathbf{A}^{-1}\mathbf{B}$ is the FD operator for the considered central node. It makes it possible to express locally the value of a stress component and its derivatives (up to the 2nd order) by the elements of the vector $\mathbf{B}$, thus by the nodal values of the stress tensor σ^k_{ij}.

For instance, the 2nd derivatives of the stresses at a Gaussian point G, required for performing integration of the curvature (5), will be expressed as

$$\begin{aligned}
&\sigma^G_{xx,xx} = 4m, \quad && \sigma^G_{xx,xy} = 6n, \quad && \sigma^G_{xx,yy} = 24p,\\
&\sigma^G_{yy,xx} = 24k, \quad && \sigma^G_{yy,xy} = 6l, \quad && \sigma^G_{yy,yy} = 4m,\\
&\sigma^G_{xy,xx} = -6l, \quad && \sigma^G_{xy,xy} = -4m, \quad && \sigma^G_{xy,yy} = -6n.
\end{aligned} \tag{21}$$

The next step performed is discretisation of the hybrid functional, Eq. (1). After building the physically based approximation at all points of interest of the considered domain, it is possible to express the hybrid functional in its discrete form. To simplify further formulae let us denote

$$\begin{aligned}
&z_1 = 2f, \quad z_2 = 2i, \quad z_3 = 6j, \quad z_4 = 2m, \quad z_5 = 3n, \quad z_6 = 12p,\\
&z_7 = 2d, \quad z_8 = 6g, \quad z_9 = 2h, \quad z_{10} = 12k, \quad z_{11} = 3l, \quad z_{12} = e.
\end{aligned} \tag{22}$$

The curvature functional, Eq. (5), may be then expressed as

$$\begin{aligned}
\Phi^{\mathrm{T}}_p &= \frac{1}{A_p}\sum_{e=1}^{N_{\text{pl}}}\sum_{i=1}^{I} w_i \left[\frac{3}{8}\left(\sigma^{eG_i}_{ij,xx}\sigma^{eG_i}_{ij,xx} + \sigma^{eG_i}_{ij,yy}\sigma^{eG_i}_{ij,yy}\right) + \frac{1}{4}\sigma^{eG_i}_{ij,xx}\sigma^{eG_i}_{ij,yy} + \frac{1}{2}\sigma^{eG_i}_{ij,xy}\sigma^{eG_i}_{ij,xy}\right] \det J_e\\
&= \frac{1}{A_p}\sum_{e=1}^{N_{\text{pl}}}\sum_{i=1}^{I} w_i \left\{5\left[\left(z_4^{eG_i}\right)^2 + \left(z_5^{eG_i}\right)^2 + \left(z_{11}^{eG_i}\right)^2\right]\right.\\
&\qquad \left. + \frac{3}{2}\left[\left(z_6^{eG_i}\right)^2 + \left(z_{10}^{eG_i}\right)^2\right] + z_4^{eG_i}z_6^{eG_i} + z_5^{eG_i}z_{11}^{eG_i} + z_4^{eG_i}z_{10}^{eG_i}\right\} \det J_e
\end{aligned} \tag{23}$$

and the experimental functional (6) as

$$\begin{aligned}
\Phi^{\mathrm{E}} &= \sum_{i,j=1}^{2}\frac{1}{K}\sum_{k=1}^{K}\frac{\left[f(\sigma^k_{ij}) - f(\bar{\bar{\sigma}}^k_{ij})\right]^2}{\Delta f(\sigma^k_{ij})^2} \qquad \textit{Czy tu i w r-niu (26) nie powinien być minus?}\\
&\qquad\qquad\qquad\qquad\qquad\qquad\qquad\qquad\qquad\qquad\qquad\qquad\qquad\qquad\qquad\qquad \downarrow\\
&= \frac{1}{K}\sum_{k=1}^{K}\left\{\frac{\left[f(z_1^k) - f(\bar{\bar{\sigma}}^k_{xx})\right]^2}{\Delta f(\sigma^k_{xx})^2} + \frac{\left[f(z_7^k) - f(\bar{\bar{\sigma}}^k_{yy})\right]^2}{\Delta f(\sigma^k_{yy})^2} + 2\frac{\left[f(z_{12}^k) + f(\bar{\bar{\sigma}}^k_{xy})\right]^2}{\Delta f(\sigma^k_{xy})^2}\right\}.
\end{aligned} \tag{24}$$

In the subsequent steps, in Eqs. (23)–(24) the z_i parameters at the Gaussian stations G_i are expressed by the nodal values of the stresses derived from the FD operator (20),

$$z_i^{eG_i} = \mathbf{A}_{ij}^{-1}\mathbf{B}\left(\sigma_j^{eG_i}\right) \tag{25}$$

and the discrete form of the hybrid functional is obtained as

$$\Phi(\sigma,\lambda) = \lambda\left\{\frac{1}{A_p}\sum_{e=1}^{N_{\mathrm{pl}}}\sum_{i=1}^{I} w_i\left[5\left(z_4^{eG_i}\right)^2 + 5\left(z_5^{eG_i}\right)^2 + 5\left(z_{11}^{eG_i}\right)^2 + \frac{3}{2}\left(z_6^{eG_i}\right)^2 + \frac{3}{2}\left(z_{10}^{eG_i}\right)^2 + z_4^{eG_i}z_6^{eG_i} + z_5^{eG_i}z_{11}^{eG_i} + z_4^{eG_i}z_{10}^{eG_i}\right]\det J_e\right\} \tag{26}$$

$$+ (1-\lambda)\frac{1}{K}\sum_{k=1}^{K}\left\{\frac{\left[f(z_1^k) - f(\bar{\bar{\sigma}}_{xx}^k)\right]^2}{\Delta f(\sigma_{xx}^k)^2} + \frac{\left[f(z_7^k) - f(\bar{\bar{\sigma}}_{yy}^k)\right]^2}{\Delta f(\sigma_{yy}^k)^2} + 2\frac{\left[f(z_{12}^k) + f(\bar{\bar{\sigma}}_{xy}^k)\right]^2}{\Delta f(\sigma_{xy}^k)^2}\right\}.$$

Imposing the necessary condition of the minimum of the functional (26) with respect to the unknown nodal values of the stress tensor $\boldsymbol{\sigma}$, a linear set of equations is obtained

$$\mathbf{H}\boldsymbol{\sigma} = \mathbf{r}. \tag{27}$$

As far as the local and global boundary conditions are concerned, Eqs. (7)–(9), they have been already partially satisfied by selection of the physically reasonable FD operators (equilibrium equations, Eq. (7)) and the rest of them, i.e., local boundary conditions, Eq. (8), and global equilibrium equations, Eq. (9), will be imposed by selection and elimination of a suitable number of the depending variables. A standard procedure of static condensation, performed after regrouping the vector $\boldsymbol{\sigma}$ to separate dependent and independent variables, will lead to the final set of linear equations expressed as

$$\mathbf{T}^{\mathrm{T}}\mathbf{H}\mathbf{T}\boldsymbol{\sigma}_{\mathrm{ind}} + \mathbf{H}\begin{bmatrix}\mathbf{0}\\ \mathbf{R}\end{bmatrix} + \mathbf{r}^T\mathbf{T} = \mathbf{0} \tag{28}$$

where $\mathbf{T}$ is a transformation matrix expressed as

$$\mathbf{T} = \begin{bmatrix}\mathbf{I}\\ -\mathbf{D}_{\mathrm{dep}}^{-1}\mathbf{D}_{\mathrm{ind}}\end{bmatrix}. \tag{29}$$

Solution to the set (29) will provide the λ-dependent stress vector σ_{ind} that fulfills all requirements imposed by internal and external equilibrium equations (7)–(9) while the two stage procedure, Eqs. (12)–(13), will guarantee that the approximated field is smooth and close to the experimentally measured values.

2.3. Estimation of a posteriori error of experimental data

The methods for a posteriori analysis of error are in particular focus in the field of the computational mechanics for more than twenty years [15] and provided a broad range of techniques suitable for this purpose. Estimates they provide are based on various mathematical foundations that mainly come from functional analysis and theory of approximation. Many different approaches emerged like e.g., implicit and explicit type residual methods, interpolation methods, post-processing methods and many other [1, 8]. They were successfully applied in the area of the FE, FD, BE and meshless methods leading to formulation and development of adaptive approaches. In opposite, in the area of experimental data analysis methods there is no matching wealth of such techniques. In fact, there are almost no such methods at all. The only methods used for years are of statistical nature [2] but

they deliver estimates of rather probability of an error than the value of the actual error. Moreover, the average estimates they deliver are often valid only for an experimental technique or the analyzed data series on the whole but on the local (point) level their analyses might be not valid.

Seemingly, there are two sources of difficulties that cause such a scarcity of a posteriori error analysis techniques for experimental data:

- error may reach almost any arbitrary level;
- it is unrelated to any rational factors or is related to random factors that are uncontrollable.

Those two sources of difficulties prohibit a simple porting of a posteriori error analysis techniques developed within the field of computational mechanics. In the case of experimental data the error estimates cannot be related e.g., to the characteristic size of an element h, approximation order p, jumps of certain derivatives j along cross-element boundaries, there are no superconvergent points present, there are no denser and coarser grids available for reference and even if they were, errors on a dense grids would not necessarily be lower than on the coarse grid.

It also very important to notice that application of the statistical methods is limited to cases when it is possible to repeat experiments for a reasonable number of times so as to collect many independent data series to build data statistics. But if either time/cost factors restrict such an approach or experiments are destructive and the sample is completely destroyed during examinations – this methodology simply cannot be applied. Also, classic least square or polynomial regression techniques [2] have their limits as they are usually formulated in such a way that the approximation base is chosen globally in the whole considered domain. This works perfectly if the investigated field conforms to the assumed base function class but might lead to significant errors if there is no such a conformance.

For these reasons a dedicated approach to estimation of experimental data *a posteriori* error is required. The basic idea that lies at the foundations of the proposed here technique is to resign from statistical modeling in favour of building high quality, physically reasonable fits to the data. Obtained in such a way enhanced field will serve as reference solution for estimation of error in a similar way that the postprocessing type methods [8, 15] use higher order solutions for error estimation.

The a posteriori estimates of experimental data error might be required for two purposes:

- to find direct local error estimates at consecutive data points that will give a measure of error present at those points, expressed preferably in the physical units valid for the considered field[11],
- to establish relative credibility of the data within a data set (called also here as internal data credibility profile).

The first of the purposes is clear and does not require explanation but the latter might not be straightforward at the first look. To explain it, let us go back to Eq. (6) and examine the meaning of the denominator $\Delta f(\sigma_{ij}^k)$. It was called then as a local weighting factor expressing relative credibility of the data at an experimental data point k and was introduced to the PBGM formulation for discrimination of "better" or "worse" data points. The more credible data points should have bigger impact on the resulting fit to the data than those less credible and the way to enforce this stipulation is simple – by introduction of local weighting factor ascribed to each data point – but it requires a relative measure of data quality, not necessarily expressed in physical units like in the case of direct local estimates of error but serving for measuring relative data credibility.

As for the first type, the simplest and most natural way of deriving such a direct local estimate is to use the GM smoothened field as a reference solution for measuring error and performing the operation on the point-by-point basis as

$$\Delta^{SBCC}\sigma_{ij} = |\sigma_{ij} - \bar{\bar{\sigma}}_{ij}|, \qquad i = 1,2, \quad j = 1,2, \tag{30}$$

[11] MPa for the case of residual stress in rails presented in the paper

where $\bar{\bar{\sigma}}_{ij}$, $i = 1, 2$, $j = 1, 2$ is experimentally measured stress field, and σ_{ij} is its respective physically based fit, and the upper index SBCC in $\Delta^{SBCC}\sigma_{ij}$ is an acronym for stress based, component-by-component error indicator.

The second type of error estimates required for building relative data credibility within a data set are proposed here as

- the relative local curvature error indicator $\Delta^{RLC}\boldsymbol{\sigma}$

$$\Delta^{RLC}\boldsymbol{\sigma} = \frac{|\kappa^2(\boldsymbol{\sigma}) - \kappa^2(\bar{\bar{\boldsymbol{\sigma}}})|}{\kappa^2(\boldsymbol{\sigma})} \tag{31}$$

where κ^2 is Karmowski's curvature of the tensor field [7], or

- the relative local gradient error indicator $\Delta^{RLG}\sigma_{ij}$

$$\Delta^{RLG}\sigma_{ij} = \frac{|\text{grad}\,(\sigma_{ij}) - \text{grad}\,(\bar{\bar{\sigma}}_{ij})|}{|\text{grad}\,(\sigma_{ij})|}, \qquad i = 1, 2, \quad j = 1, 2. \tag{32}$$

Both the indicators (31) and (32) are devised to reveal the areas/points where the most intensive physically based smoothing took place. Because first and second order derivatives of the stress field are used in those definitions, but not the values of the stresses themselves, the estimates built with their help with ease separate areas of rapidly changing stress components (i.e. where smoothing is intensive) and make it possible to built the internal data credibility profile without finding the final value of the parameter λ[12]. The $\Delta^{RLC}\sigma$ indicator provides a combined estimate for all three stress components at a point while the $\Delta^{RLG}\sigma_{ij}$ indicator works in a more subtle way, discerning the differences between the stress components. It is perhaps worth pointing out here that, theoretically, the SBCC derived error estimates might also serve for this purpose but one must be aware of the fact that the values of the stress components are strongly dependent on the current value of the parameter λ, so to find a good estimate of the internal data credibility profile it would be required that the final fit to the data is known, which in return calls for a proper internal data credibility profile.

3. Exemplary results

The PBGM approach was under development for the last several years and many tests and benchmarks were performed for its validation and tuning. Here only exemplary results will be recalled for illustration of the performance of the data smoothing/enhancement technique. A benchmark case for generated pseudo-experimental data will be shown first and then error analysis of the nowadays classic in the field J.J. Groom [4] strain gauge data for residual stress in railroad rails will be performed.

3.1. Tests for elliptic plate

Firstly, let us consider an elliptic plate with a stress field generated by the stress function approach. The stress function has the nonlinear form as

$$\text{F(x,y)} = 2\,\frac{1 - \cos(\vartheta b(x, y))}{\vartheta^2} \tag{33}$$

[12]or, in exchange, the final fit to the stress field

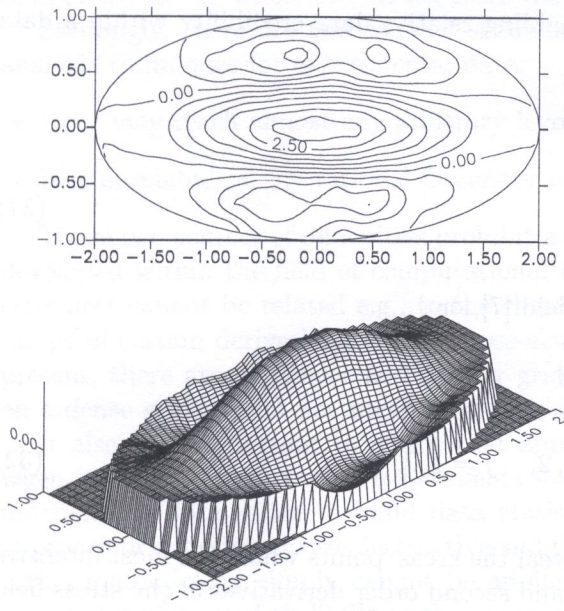

Fig. 1. Elliptic plate. Generated σ_{xx} stress component

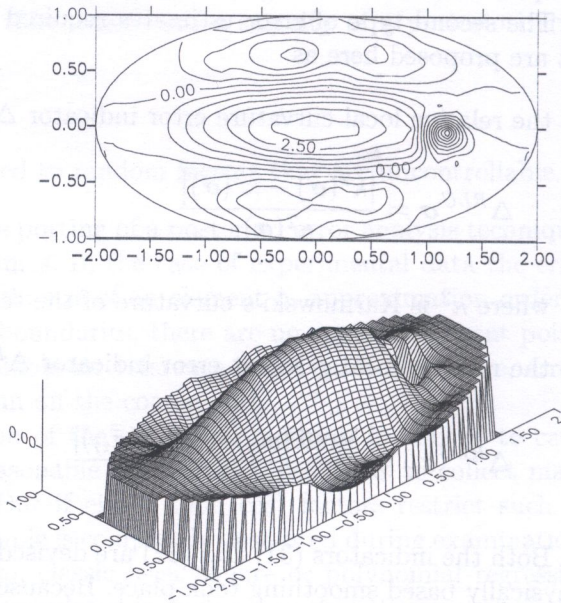

Fig. 2. Elliptic plate. Disturbed field for σ_{xx} stress component

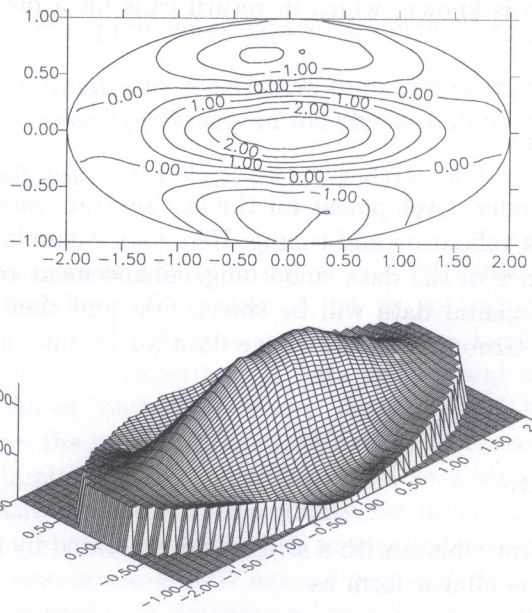

Fig. 3. Elliptic plate. Smoothened field for σ_{xx} stress component

with the degree of nonlinearity controlled by the parameter ϑ. The function $b(x, y)$ in Eq. (33) is the function describing the boundary of the ellipse,

$$b(x,y) = \left(\frac{x}{a_x}\right)^2 + \left(\frac{y}{a_y}\right)^2 - 1, \qquad a_x = 1, \quad a_y = 2. \tag{34}$$

In this benchmark, the pseudo-experimental data was generated with the use of the function $F(x, y)$, Eq. (33) over a random set of 50 data points and was further manually perturbed, but only for one stress component and at only one point. In Fig. 1 an intact data is shown, in Fig. 2 after perturbation was introduced. The stress component which was perturbed was the σ_{xx}, the coordinates of the point of perturbation were $P(0.116666\text{E}{+}01, -0.277885\text{E}{-}01)$. The original value of σ_{xx} at that point was ca. 1.0401 and it was disturbed to ca. -4.489.

A smoothened with PBGM solution is shown in Fig. 3, in Fig. 4a a map of exact error is plotted whereas in Fig. 4b the PBGM SBCC error estimate. As it may be seen, the PBGM-derived error estimate is excellent all over the elliptic area, even though it exhibits minor fluctuations visible in the plot, Fig. 4b. What is important here – and was the main reason for performing so simple a test – is the observation that the PBGM procedure, performing pretty complex constrained optimisation, worked with very high precision in the area of error and left the rest of the filed almost intact, save the slight fluctuations (noise) in the patterns, but they are of negligible amplitude.

Quantitative analysis of error renders absolute error as 5.53 (exact) in opposite to 5.49 estimated by GM-based error estimate procedure. Relative values of error are 531.79% vs. 527.85%, respectively, thus the GM procedure estimate missed the exact value by 0.74%.

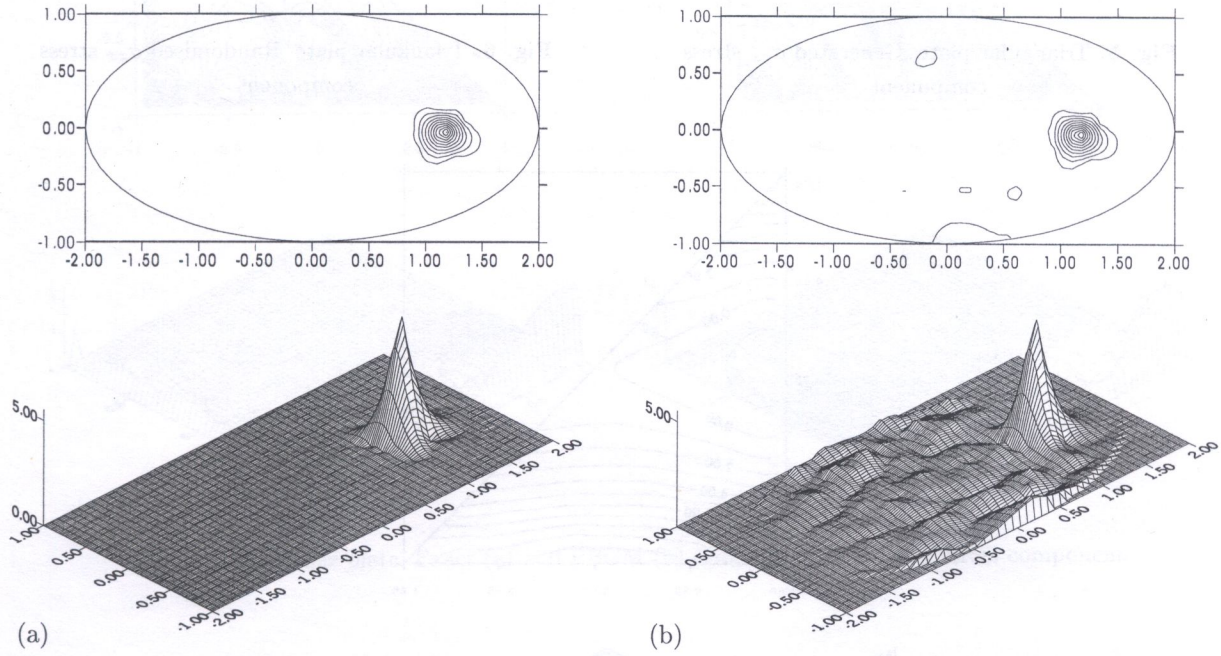

Fig. 4. Exact (a) and PBGM (b) error estimates for σ_{xx} stress component

3.2. Tests for triangular plate

The first test was simplistic, it demonstrated that the PBGM smoothing may constitute a base for building the reference fields and further post-processing type, non-statistical experimental data error estimates, but the assumed simplifications made this test afar from usual experimental data quality and its error distributions. Now let us consider a more "standard" data behaviour, where all stress components over a triangular domain was subject to randomisation with amplitude of 20%.

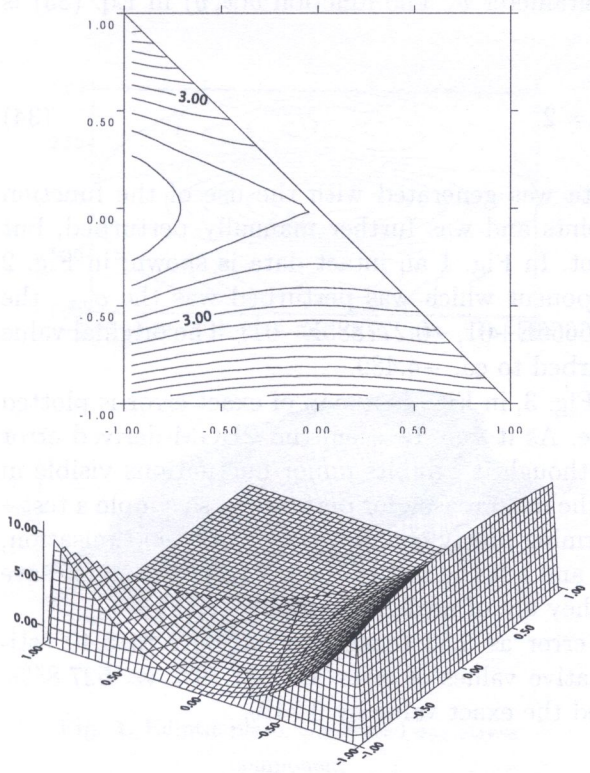

Fig. 5. Triangular plate. Generated σ_{xx} stress component

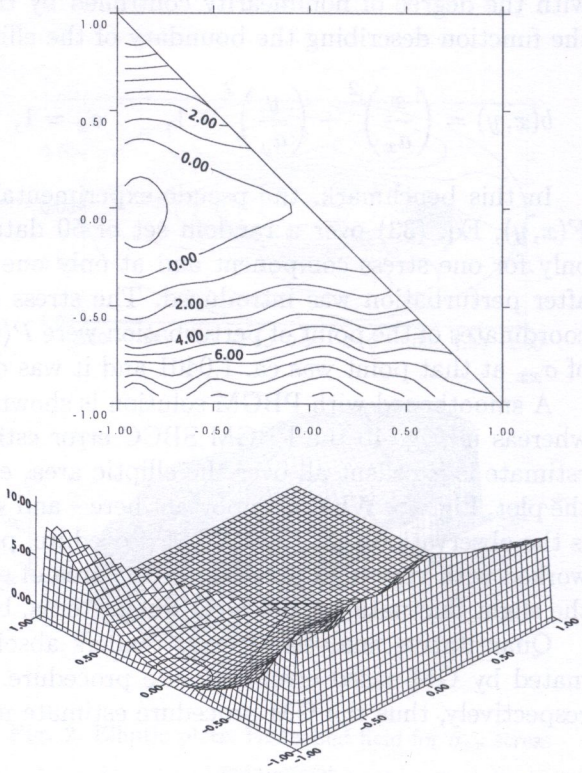

Fig. 6. Triangular plate. Randomised σ_{xx} stress component

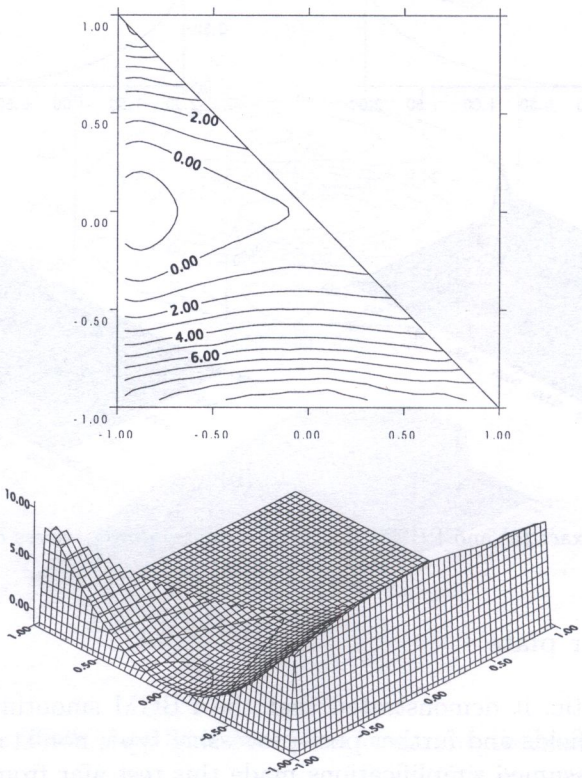

Fig. 7. Triangular plate. PBGM smoothened σ_{xx} stress component

Considered is a triangular plate for each distribution of the stress function was assumed as a fourth order polynomial,

$$F(x,y) = 3x^4 + y^4 - x^2y^2 - 3x^2. \tag{35}$$

The stress components are thus defined as

$$\sigma_{xx} = 12y^2 - 2x^2, \qquad \sigma_{yy} = 36x^2 - 2y^2 - 6y, \qquad \sigma_{xy} = 6x - 4xy. \tag{36}$$

In Fig. 5 the patterns of the σ_{xx} stress component are shown[13], after randomization they are portrayed in Fig. 6, PBGM smoothing renders them back as shown in Fig. 7. In Fig. 8 distributions of the exact error (Fig. 8a) and its PBGM estimate (Fig. 8b) are shown. The PBGM error estimate shows a very good agreement with the exact error distribution in the internal parts of the domain (they differ by 3–5%), suffering only at the boundaries, where it misses the exact error measure by 10–12%.

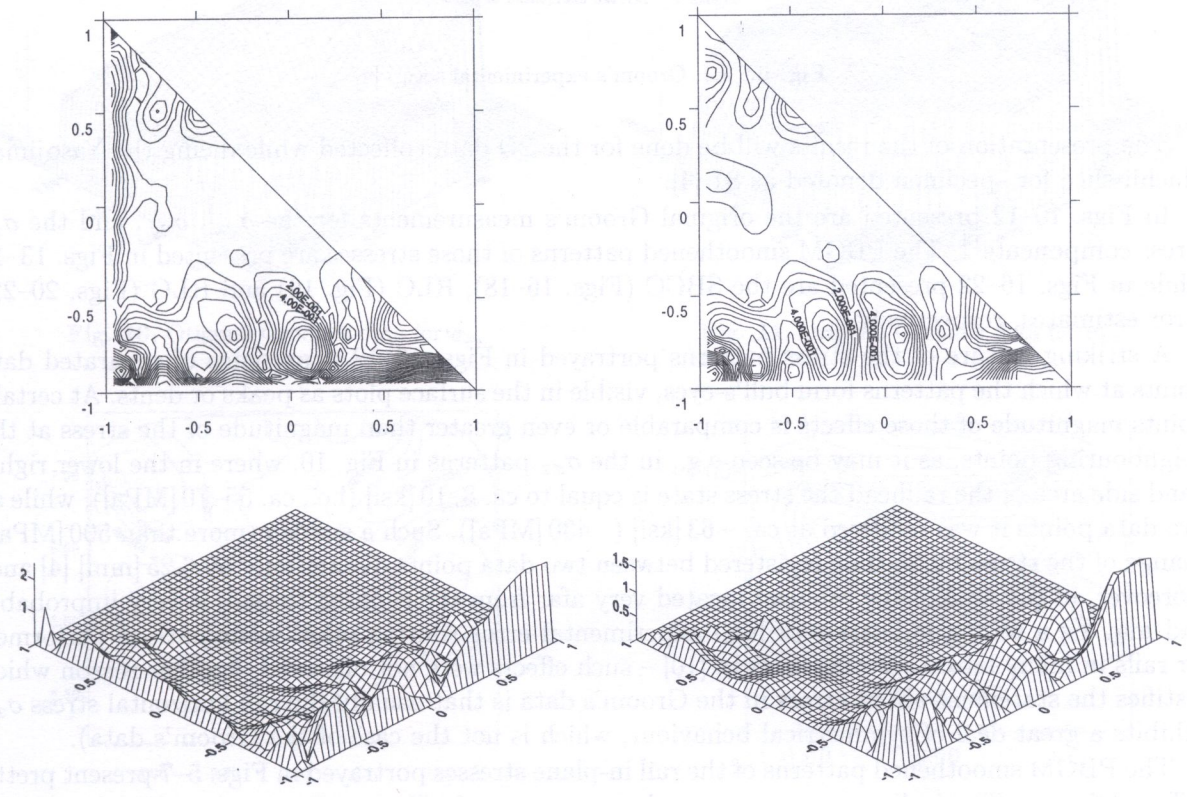

Fig. 8. Triangular plate. Exact (a) and PBGM (b) error estimates for σ_{xx} stress component

3.3. Tests for a railroad rail data

The J.J. Groom's [4] data for rails has been considered over many years as the most accurate and credible source data for distribution of residual stress in railroad rails. Results were obtained by the strain gauge technique in the course of destructive testing performed by removal of two samples out of each rail specimen:

- a thin slice called as Yasojima–Machii samples ,
- a ca. 0.5 m long Meier section, Fig. 9.

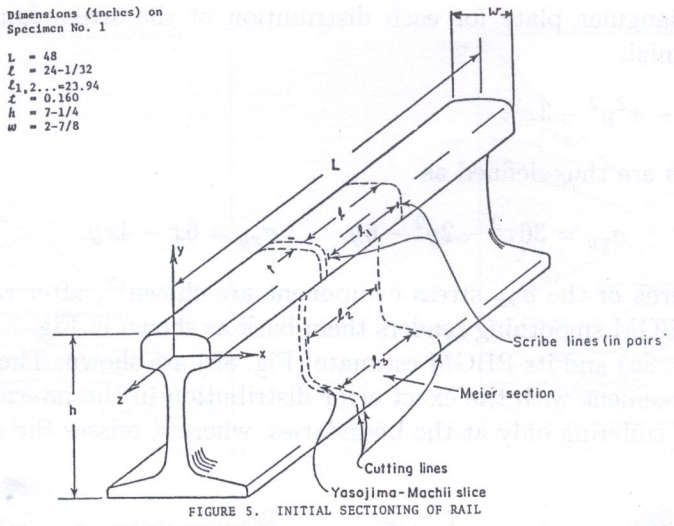

FIGURE 5. INITIAL SECTIONING OF RAIL

Fig. 9. J.J. Groom's experimental setup [4]

The presentation of the results will be done for the 2D data collected while dicing the Yasojima–Machii slice for specimen denoted as S1 [4].

In Figs. 10–12 presented are the original Groom's measurements for the σ_{xx}, σ_{yy}, and the σ_{xy} stress components[14]. The PBGM smoothened patterns of those stresses are presented in Figs. 13–15 while in Figs. 16–22 presented are the SBCC (Figs. 16–18), RLC (Fig. 19) and RLG (Figs. 20–22) error estimates, respectively.

A striking feature of the stress patterns portrayed in Figs. 10–12 is presence of separated data points at which the patterns form bull's-eyes, visible in the surface plots as peaks or dents. At certain points magnitude of those effects is comparable or even greater than magnitude of the stress at the neighbouring points, as it may be seen e.g., in the σ_{xx} patterns in Fig. 10, where in the lower right-hand side area of the railhead the stress state is equal to ca. 8–10 [ksi] (i.e., ca. 55–70 [MPa]), while at two data points it was rendered at ca. -63 [ksi] (-430 [MPa]). Such a sudden (more than 500 [MPa]) change of the stress magnitude registered between two data points distant only by 6.25 [mm] [4] and, moreover, in the area of the railhead located very afar from the running thread, is very improbable and may be a strong indication of high experimental error (during other examinations performed for rails in many labs – see references in [10] – such effects were not observed; another reason which justifies the statement about errors in the Groom's data is that usually the rail horizontal stress σ_{xx} exhibits a great deal of symmetrical behaviour, which is not the case of the Groom's data).

The PBGM smoothened patterns of the rail in-plane stresses portrayed in Figs. 5–7 present pretty different image. The isolines are now smooth, no cusps or bull's-eyes are present. The horizontal stress σ_{xx} regained its symmetry, being rendered as tensile interior and compressive exterior. The vertical stress σ_{yy} forms now a kind of triangular tensile region in the midst of the head and bands of strong compressive stress located at the vertical sides of the head. The extreme stresses are located on the gage side of the rail. The shear stress component σ_{xy} was rendered with its characteristic [10] anti-symmetrical behaviour (as regards areas of tension and compression).

Analysis of error estimates data in Figs. 16–22 clearly proves that there are two subsets in the original strain gage data: the first one of good quality that produces flat areas in the surface plots in Figs. 16–22 and the second one, counting several data points, where errors are very high. They form several very steep peaks in the surface plots. As it may be seen, all the proposed error estimates (direct SBCC error norms and RLC/RLG error norms) were able to spot those data points correctly.

[13] for the sake of brevity, the other components were again skipped

[14] in order to have ability of direct comparisons with the original Groom's work, the original units [ksi] used in [4] were preserved; please note that 1 [ksi] $\approx$ 6.9 [MPa]; all data is given both in American ans SI units

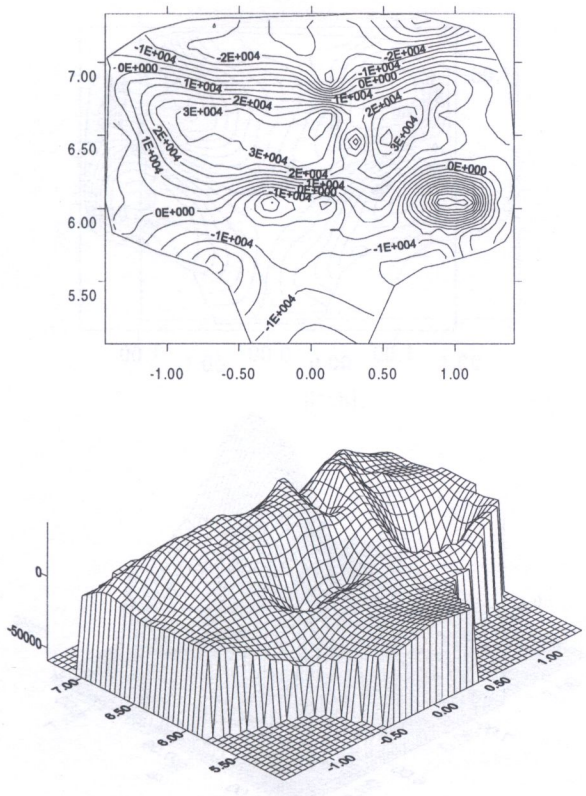

Fig. 10. Original Groom's data for σ_{xx}

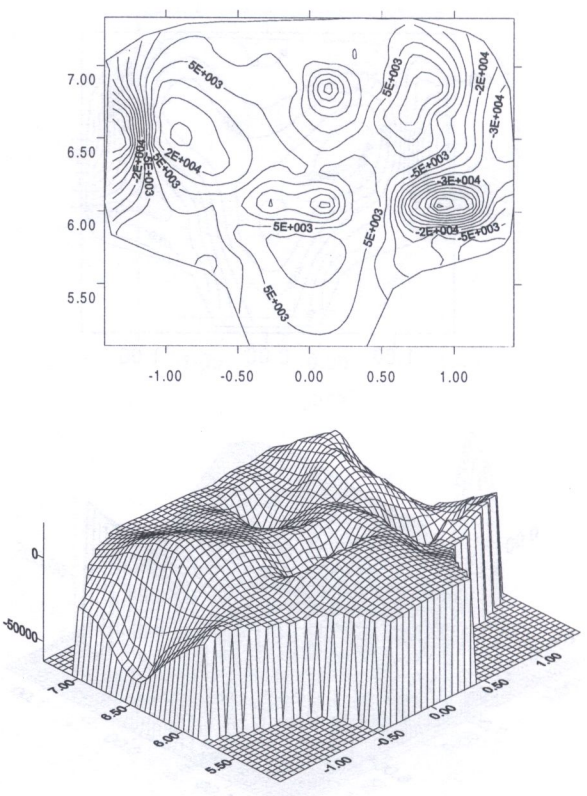

Fig. 11. Original Groom's data for σ_{yy}

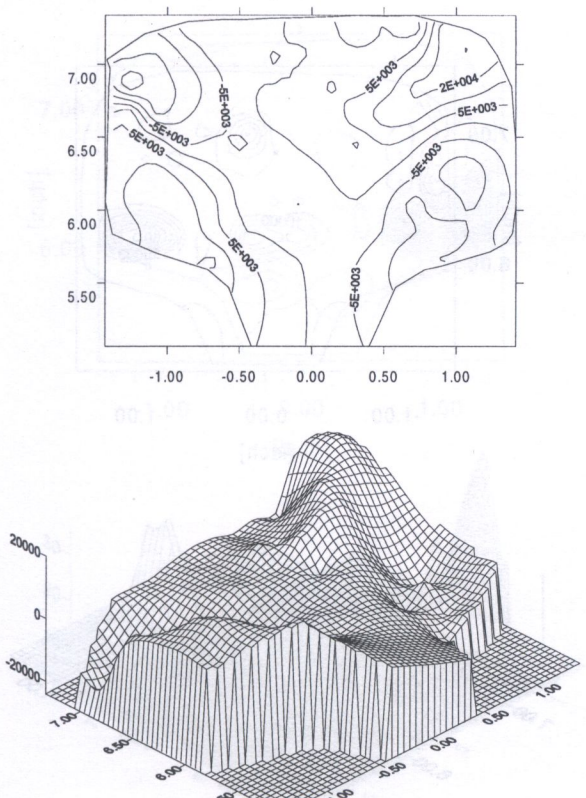

Fig. 12. Original Groom's data for σ_{xy}

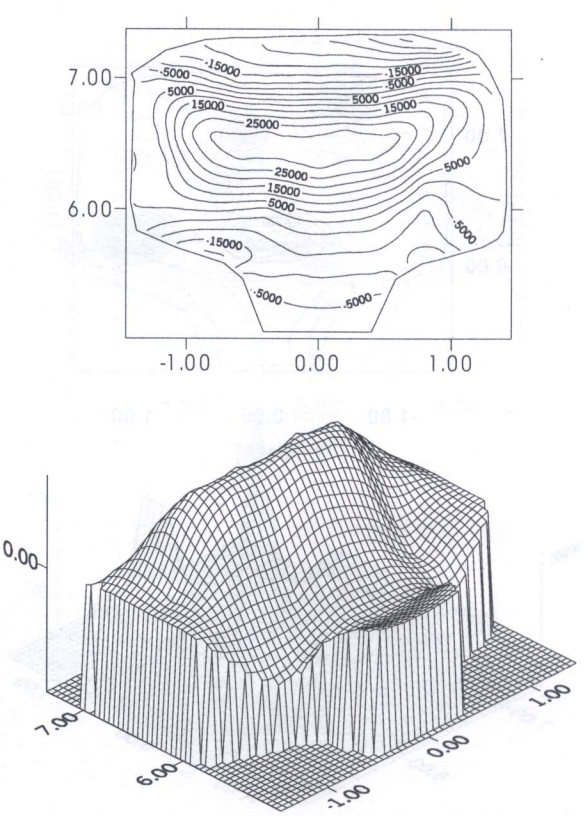

Fig. 13. GM smoothened Groom's data for σ_{xx}

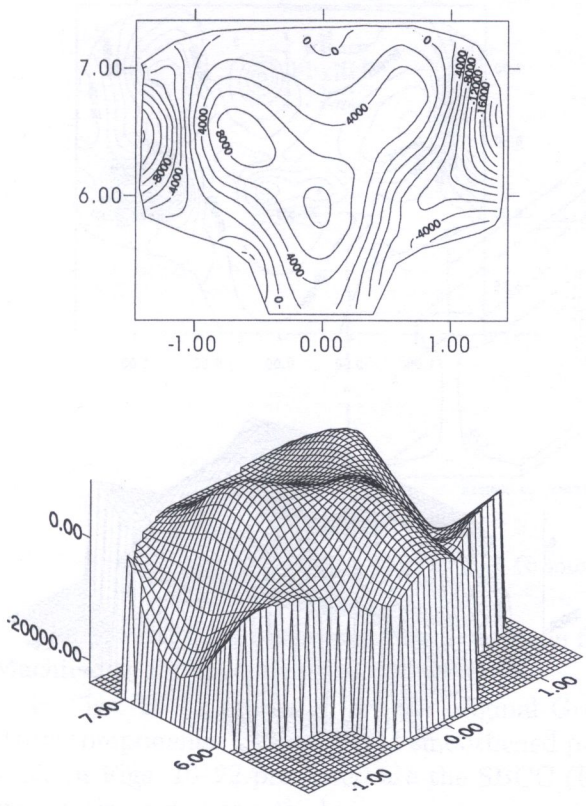

Fig. 14. GM smoothened Groom's data for σ_{yy}

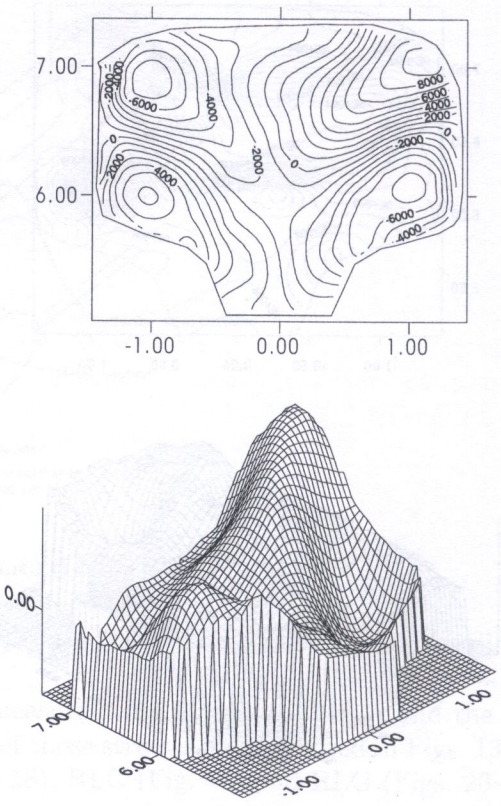

Fig. 15. GM smoothened Groom's data for σ_{xy}

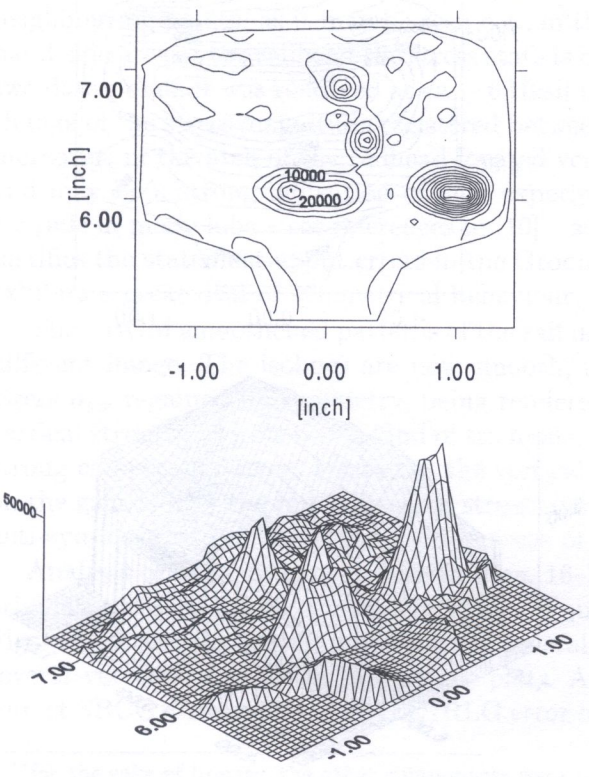

Fig. 16. Error estimate for σ_{xx}, SBCC approach

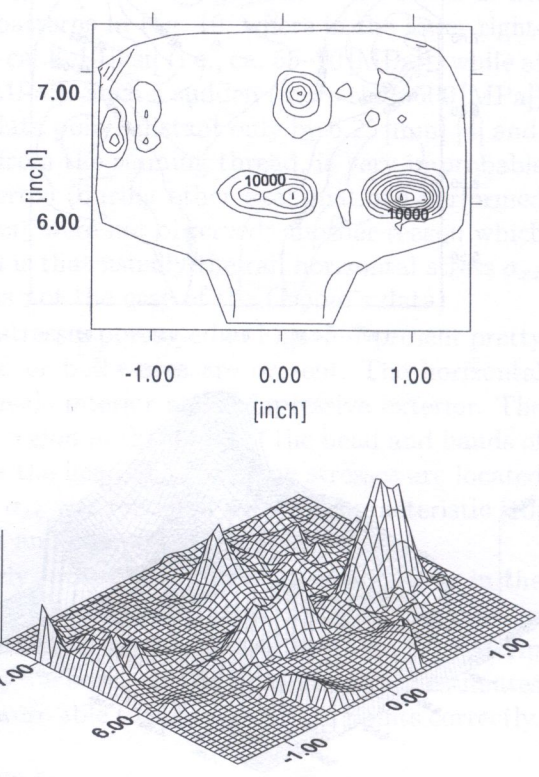

Fig. 17. Error estimate for σ_{yy}, SBCC approach

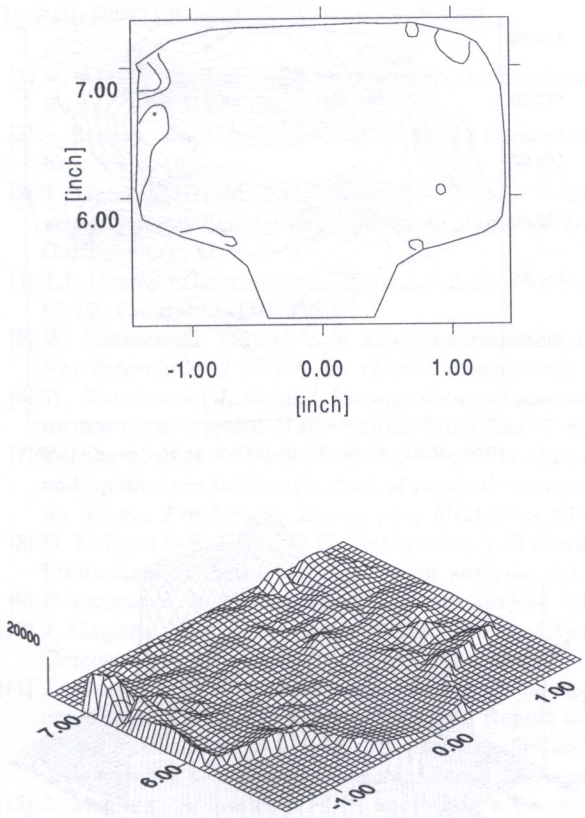

Fig. 18. Error estimate for σ_{xy}, SBCC approach

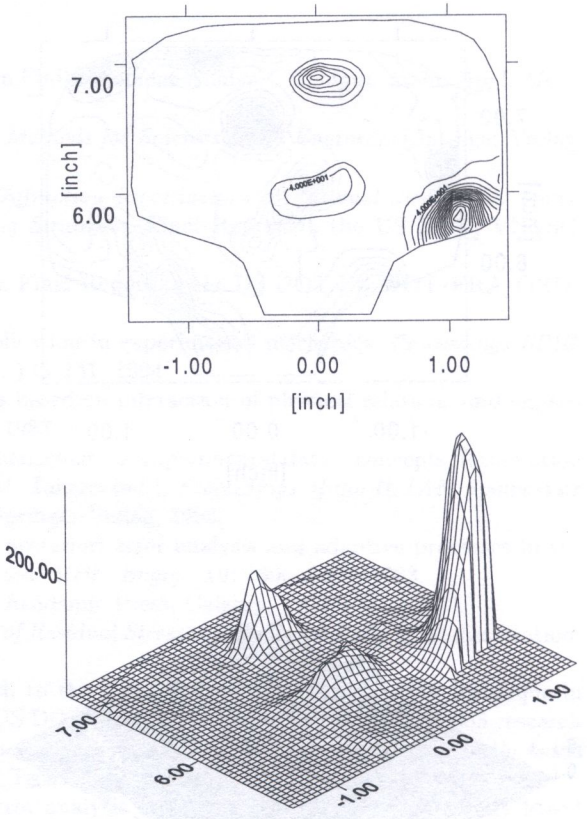

Fig. 19. Error estimate for σ, RLC approach

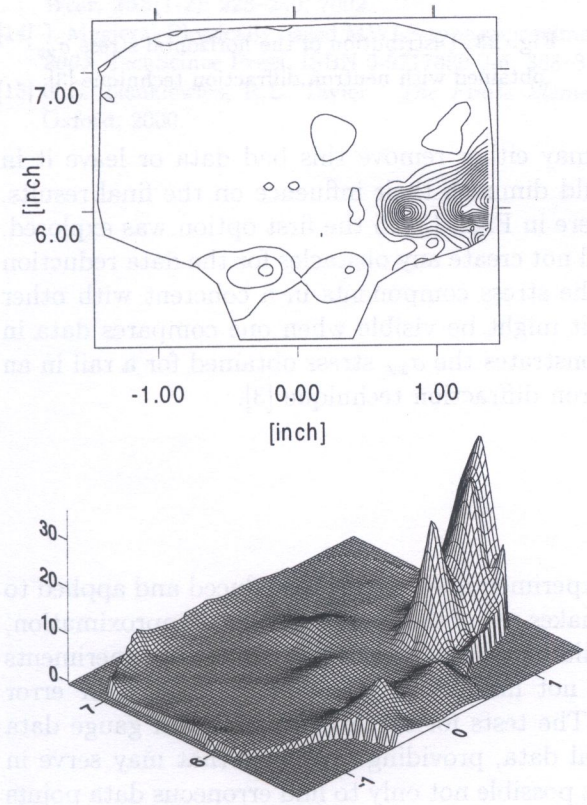

Fig. 20. Error estimate for σ_{xx}, RLG approach

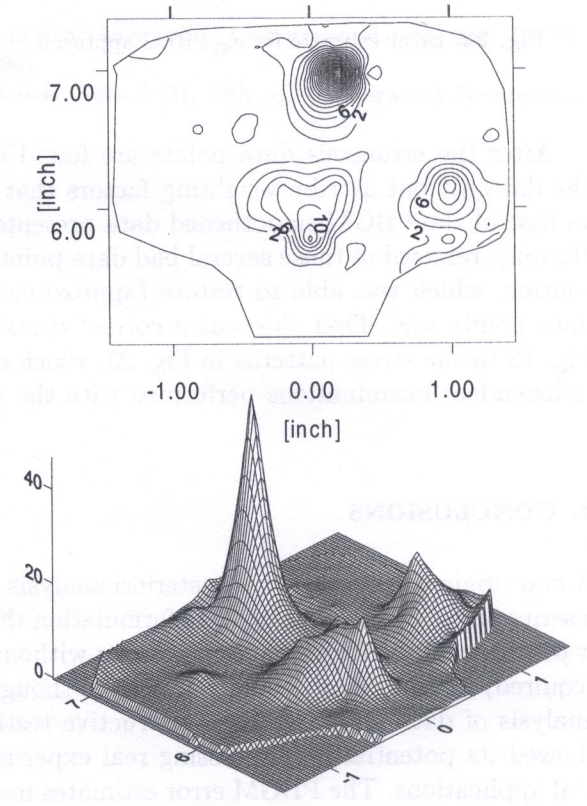

Fig. 21. Error estimate for σ_{yy}, RLG approach

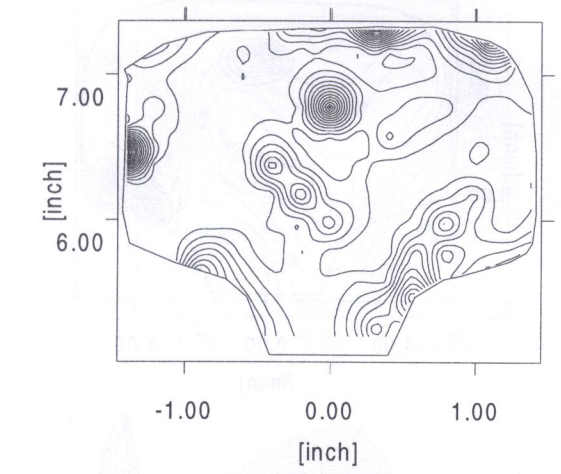

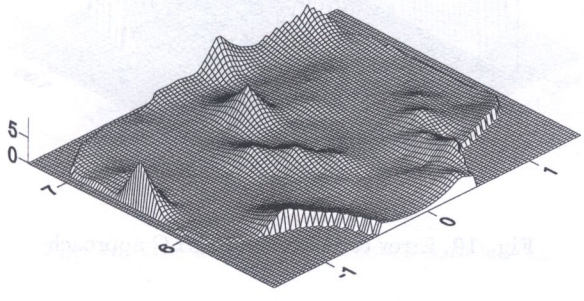

Fig. 22. Error estimate for σ_{xy}, RLG approach

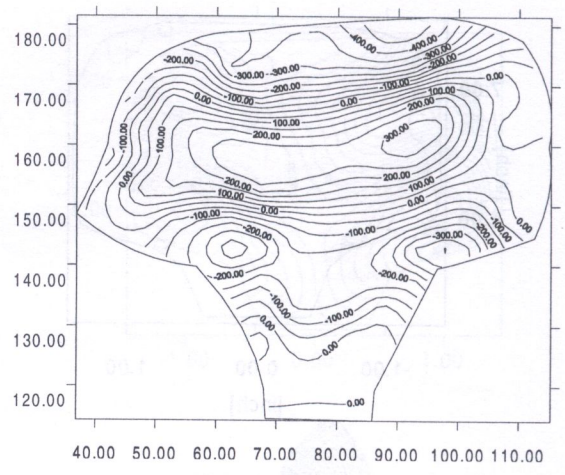

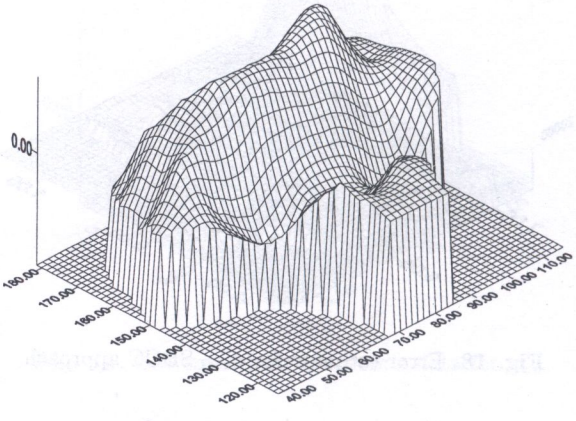

Fig. 23. Distribution of the horizontal stress σ_{yy} obtained with neutron diffraction technique [3]

After the erroneous data points are found one may either remove this bad data or leave it in the data set but ascribe weighting factors that would diminish their influence on the final results. In case of the PBGM smoothened data presented here in Figs. 13–15 the first option was explored. Happily, removal of those several bad data points did not create any obstacles for the data reduction routine, which was able to restore (approximate) the stress components in a coherent with other data points way. That this was a correct decision, it might be visible when one compares data in Fig. 13 to the stress patterns in Fig. 23, which demonstrates the σ_{xx} stress obtained for a rail in an independent examinations performed with the neutron diffraction technique [3].

4. Conclusions

A new original approach to a posteriori analysis of experimental error was introduced and applied to a series of data sets. Thanks to its formulation that makes use of the physically based approximation, it provides means for estimation of error without building data statistics (no repetitive experiments required) thus it may lend itself well – though is not limited to – for smoothing and/or error analysis of data obtained from destructive testing. The tests for the exemplary strain gauge data showed its potential for processing real experimental data, providing estimates that may serve in real applications. The PBGM error estimates make it possible not only to find erroneous data points but to build its credibility profile, which make it possible to extend further the approach into smart smoothing procedure that employs smoothing with a localized, error controlled intensity.

REFERENCES

[1] M. Ainsworth, J.T. Oden. A posteriori error estimation in Finite Element Analysis. *Comput. Meth. Appl. Mech. Engrg.*, **142**: 1–88, 1997.

[2] S. Brandt. *Data Analysis. Statistical and Computational Methods for Scientists and Engineers.* Springer-Verlag, New York, 1999.

[3] T. Gnäupel-Herold, P.C. Brand, H.J. Prask. *Neutron Diffraction Investigation of Residual Stresses in Transverse/Oblique Rail Slices subjected to Different Grinding Strategies.* Final Report to the US DOT, VNTSC, Gaithersburg, MD, 1998.

[4] J.J. Groom. *Determination of Residual Stresses in Rails.* Final Report to the US DOT No. DOT/FRA/ORD–83/05, Columbus, OH, 1983.

[5] W. Karmowski. Global–local approximation and its application in experimental mechanics. *Proceedings SPIE, The International Society for Optical Engineering*, **2342**: 135–141, 1994.

[6] W. Karmowski, J. Orkisz. Fitting of curves and surfaces based on interaction of physical relations and experimental data. *Applied Mathematical Modelling*, **7**: 65–69, 1983.

[7] W. Karmowski, J. Orkisz. Physically based method of enhancement of experimental data – concepts, formulation and application to identification of residual stresses. In: M. Tanaka (ed.), *Proceedings of the IUTAM Symposium on Inverse Problems in Engineering Mechanics*, 61–70. Springer-Verlag, 1993.

[8] D. Kelly, J.D.S. Gago, O.C. Zienkiewicz, I. Babuska. A posteriori error analysis and adaptive processes in the Finite element method. Part I – error analysis. *Int. J. Num. Meth. Engrg.*, **19**: 1596–1619, 1983.

[9] P. Lancaster, K. Salkauskas. *Curve and Surface Fitting.* Academic Press, Calgary, 1990

[10] J. Magiera. *Hybrid Experimental and Numerical Analysis of Residual Stresses in Railroad Rails.* PhD dissertation, Cracow University of Technology, Cracow, 2001.

[11] J. Magiera. Further development of the global approach to the physically based approximation technique in experimental analysis of residual stresses, Report to the US DOT, FRA under the DTFR53-95-G-00055 research project *Development of advanced methods for the prediction of shakedown stress states and physically based enhancement of experimental data.* Cracow University of Technology, Cracow, 2002.

[12] J. Magiera. A meshless FDM applied to a posteriori error analysis of experimental data by physically based global method approximation. In K.J. Bathe (ed.), *Computational Fluid and Solid Mechanics. Proc. 2nd MIT Conference*, 2060–2063. Elsevier, 2003.

[13] J. Magiera. Enhanced 3D analysis of residual stress in rails by physically based fit to neutron diffraction data. *Wear*, **253**(1-2): 228–240, 2002.

[14] J. Magiera. Physically based MWLS-type approximations in smart smoothing of experimental data. *Proc. ICCES 2005*, TechScince Press, ISBN 0-9717880-0-6, 308–313, 2005.

[15] O.C. Zienkiewicz, R.L. Taylor. *The Finite Element Method*, Vols. I–III, fifth ed. Butterworth-Heinemann, Oxford, 2000.